Mathematics

AIMS Mathematics, 11(5): 14820–14839.
DOI: 10.3934/math.2026610
Received: 05 March 2026
Revised: 22 April 2026
Accepted: 28 April 2026
Published: 26 May 2026

https://www.aimspress.com/journal/Math

Research article

Mathematical and numerical modeling of drilling system dynamics using CF fractional differentiation

Mahir Ceylan ERDOĞAN*

Department of Computer Engineering, Istanbul Health and Technology University, Istanbul, Turkey

* **Correspondence:** Email: erdoganmahir@gmail.com; Tel: +905354047920.

Abstract: In this work, I propose a Caputo–Fabrizio fractional mathematical model of a drilling system (CFFMMDS) to investigate the coupled dynamics of an induction motor-driven drilling assembly within a unified fractional-order framework. The governing equations were formulated using a nonsingular Caputo–Fabrizio fractional derivative with an exponential memory kernel to characterize the temporal dependencies among the system state variables. The resulting fractional-order system was solved using the Caputo–Fabrizio q-Elzaki homotopy analysis transform method (CFq-EHATM) to derive semi-analytical solution series and to conduct a numerical investigation of the system response under varying fractional orders. The results indicated that a decrease in the fractional order μ results in attenuated growth and decay rates. This trend is consistent with the intrinsic memory structure of the Caputo–Fabrizio operator, which distributes the influence of past states over time. The proposed framework enables the analysis of the temporal evolution of coupled state variables in dynamic systems exhibiting history-dependent behavior.

Keywords: Caputo–Fabrizio fractional derivative; drilling system dynamics; mathematical modelling
Mathematics Subject Classification: 34K37, 34N05, 35R07

1. Introduction

Rotary drilling systems are intricate, multi-component mechanical systems that are commonly used in drilling operations and are known for being inherently complex and dynamic [1,2]. This complexity arises from the continuous interaction and force transmission occurring between the drill bit, bottom-hole assembly components, drill string, and surface equipment [3]. Although drilling

systems may operate smoothly under uniform conditions, uncontrollable formation parameters, such as variations in rock hardness or softness, often induce irregularities in torque transmission [4]. Therefore, stick-slip oscillations or chaotic rotational responses may emerge during drilling operations [5,6]. Figure 1 shows the standard drilling components.

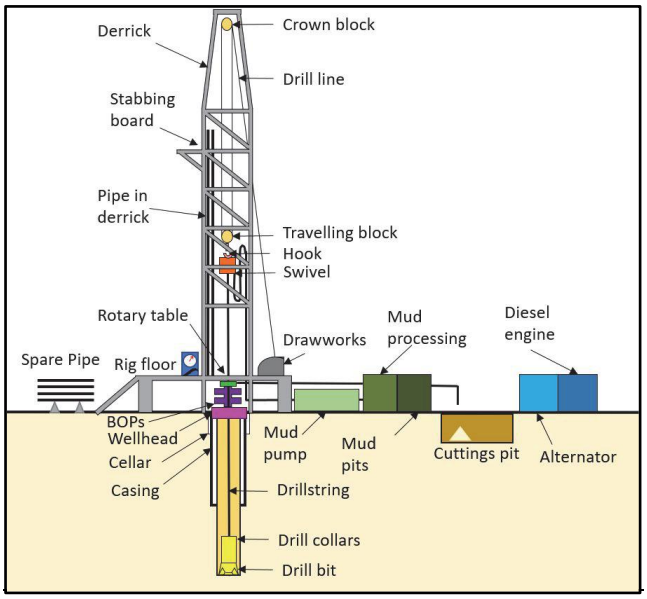

Figure 1. General schematic of standard drilling components [7].

Such chaotic behaviors are undesirable to contractors and operators, as they result in significant system level and operational problems and additional operational costs [7,8]. Torque transmission variation results in intermittent cutting, and as a result, a significant portion of the mechanical energy supplied is dissipated as vibrations rather than being transferred to rock fragmentation [9,10]. Consequently, the mechanical specific energy necessary to achieve the target depth is increased, the penetration rate decreases and, because of the sudden changes in the loading, drill bits become delaminated, causing microcrack formation, which reduces the service lifetime [10,11]. In extreme cases, these instabilities can result in drill-string buckling or failure, downhole tool malfunctions, and prolonged non-productive time [11].

Different vibration modes are encountered due to drilling operations, and these are generally arranged into three basic forms: lateral, axial, and torsional [12]. Of these, torsional vibration is considered the most dangerous and damaging, as it is most closely related to the occurrence of stick-slip motions [13]. These oscillations may produce sudden spikes in torque or excessive torsional loading, resulting in failure of the drill bit, cracking at the connection regions of bottom-hole assembly components, buckling of the drill string, sensor failures inside the BHA, and the excitation of coupled axial and lateral vibrations [13].

Studies [14,15] have shown that the nonlinear forces caused by bit-formation interaction, including friction, which increases as angular velocity decreases, are the principal mechanisms of self-excited torsional vibrations and dynamic irregularities. Researchers [16,17] have stated that using the constant angular velocity at the drilling platform of a drilling system, nonlinear dynamic characteristics of drill strings cause limit cycles, bifurcations, and chaotic attractors. Although these works offer important insights into the mechanisms of dynamic instabilities in drilling operations, the memory effects addressed in such works are mostly confined to delay-based kinematic formulations. However,

the hereditary memory behavior due to friction and damping mechanisms along the drill string has yet to be sufficiently studied.

In practice, well-defined legacy effects of the hereditary nature of drilling systems can be seen primarily due to different elasticities on varying distances along the drill string, bit-rock interaction-caused frictional hysteresis, and complicated downhole boundary conditions [18,19]. Long-run energy release and accumulation are experienced in the system, and nonlinearity of the motion, characterizing the motion, friction-slip behavior, for example, demonstrates the presence of intrinsic delay of time to generate the load [20]. Traditional integer order derivatives can capture only short-term dynamics and are therefore insufficient for modeling memory effects [21–23].

Traditional equations therefore fail to capture the timing or suppression of torsional oscillations, like stick-slip behavior, correctly [24]. In recent years, fractional calculus has become a more powerful mathematical theory for the modeling of dynamic systems with memory effects, nonlocal interactions, and nonlinear damping [25]. However, in comparison to classical derivatives, fractional derivatives can show historical system behavior in integral kernels because they make an ideal time dependent mechanical and geomechanical process more transparent [26]. However, the Caputo–Fabrizio fractional derivative has received more attention because of its nonsingular kernel [27,28]. It is also preferred for its exponential memory structure [29]. These properties have made it attractive in many recent studies [30,31].

In this work, we deal with the nonphysical singularities of the nonphysical fractional derivatives but maintain a proper and consistent memory model.

Fractional derivatives in their modern form include Riemann–Liouville, Caputo, and Atangana–Baleanu, among others. Some traditional definitions, like Riemann–Liouville and Caputo derivatives, use singular power-law kernels to derive their derivatives, which may be problematic from an interpretative perspective and in the numerical one. On the other hand, the Caputo–Fabrizio fractional derivative is written as a non-singular exponential kernel that removes the singularity at the origin, giving better numerical stability. This property makes it especially well-suited to models with fading memory and where smooth kernel behavior is desirable.

Non-singular fractional operators have attracted significant attention due to their ability to incorporate memory effects without the singular kernels present in classical fractional derivatives. In particular, operators such as the Caputo–Fabrizio formulation provide improved numerical stability and physical interpretability by avoiding power-law singularities. Researchers have focused on the development of efficient numerical techniques for such models, including decomposition-based and collocation methods. For example, Baleanu and Shiri [32] presented a numerical framework for fractional Neumann series equations, demonstrating reliable convergence and stability. These developments highlight the growing importance of non-singular fractional operators in theoretical analysis and numerical computation.

In an experimental setting, the Caputo–Fabrizio operator has been successfully used in a number of areas such as heat transfer and anomalous diffusion [33–35]. It has also been applied to control systems [36,37]. Additionally, it has been used in modeling viscoelastic material models, with strong agreement on damping and relaxation behaviors [38,39].

In mechanical systems, fractional derivatives model instantaneous and history-dependent mechanisms of energy dissipation [40]. Because of its slender and distributed-parameter construction, drill strings experience large stick-slip torsional vibrations, frictional memories, and complex inertial–elastic interactions [41]. Therefore, many characteristic properties that are hard to represent using the classical derivative-based models can be effectively described by a fractional-order formula [42]. Studies have shown that fractional models do considerably enhance the performance in dynamic

prediction for damping dominated mechanical systems [43,44].

The friction-related limit cycles, nonlinear force interactivity, and energy-based stability criteria were investigated in the prior drilling dynamics work, though fractional derivative-based methods have been somewhat less studied [45]. Novel works [46,47] demonstrated nonsingular fractional operators, in particular fractal-fractional operators, for modeling nonlinear systems that usually show a large memory influence. The two works provided a methodological basis for the implementation of Caputo–Fabrizio-based operators in deep history-based mechanical systems such as drilling assemblies. The Caputo–Fabrizio operators are a good framework to assimilate the hereditary effects in torsional-electromechanical drilling dynamics studied in this work, as it has a nonsingular exponential memory kernel with an easily applied implementation [48].

While the integer-order formulation in the considered model has been analyzed before by Abro and Atangana [49], I substantially advance this framework in several key steps. First, in the application of the Caputo–Fabrizio derivative, the classical model is generalized for a fractional-order structure where memory effects not captured in integer-order systems may be taken into consideration. Second, a novel hybrid analytic technique, the conformable q-Elzaki homotopy analysis transform method (CFq-EHATM), is proposed to obtain approximations of solutions for the resulting fractional system. Notably, in contrast to the work available, I not only present a more general formulation but also propose an efficient solution methodology and study the influence of the fractional-order parameter on system dynamics. As a result, this study adds to the literature, methodologically and analytically.

In this work, I obtain a Caputo–Fabrizio fractional mathematical model of the drilling system (CFFMMDS) to analyze the system's components dynamics in the framework of fractional-order differential. The nonsingular exponential kernel of the Caputo–Fabrizio fractional operator is applied to the governing equations of the induction motor–driven system, including in a fractional derivative representation for a mathematically defined temporal dependence between state variables. The obtained fractional-order system is solved using the CFq-EHATM to derive semi-analytical solution series and numerically interpret the response of the solution at a different fractional order. It should be noted that the Caputo–Fabrizio fractional derivative employed in this study is used in its standard form. The novelty of this work lies in its application within the proposed CFq-EHATM framework and its use in modeling drilling system dynamics. This framework enables a parametric study of the effect of the fractional order μ on the temporal evolution of the solution space, providing a formal mathematical basis for the analysis of history-dependent dynamic systems.

2. The major definitions and the semi-analytical mathematical method

In this section, the major definitions of CFFC and Elzaki transform (ET) are provided.

Definition 2.1. Assume that $\sigma(t) \in C^1[0,T]$. This ensures the existence of $\sigma'(\tau)$ and the well-posedness of the integral operator. The CFFD of order $\mu > 0$ for $\sigma(t)$ is identified as [50,51]:

$$ {}^{CF}_{t_0}D^{\eta}_{0,t}[\sigma(t)] = \frac{\varpi(\mu)}{1-\mu}\int_0^t \sigma'(\tau)\, exp\left[-\frac{\mu(t-\tau)}{1-\mu}\right] d\tau, \tau > 0 \quad (1) $$

where, $\boldsymbol{\varpi(\mu)}$ denotes the normalization function associated with the Caputo–Fabrizio fractional derivative. This function is introduced to preserve consistency with the classical integer-order derivative in the limiting cases and is commonly chosen such that $\boldsymbol{\varpi(0) = \varpi(1) = 1}$.

Definition 2.2. The Elzaki transform is defined for function of exponential order. I consider functions in the set $\boldsymbol{A}$ defined by

$$\boldsymbol{A}=\left\{\boldsymbol{\sigma(t)}:\exists \boldsymbol{M},\boldsymbol{\nu_1},\boldsymbol{\nu_2}>\mathbf{0},|\boldsymbol{\sigma(t)}|<\boldsymbol{Me^{\frac{|t|}{\nu_s}}},\boldsymbol{if}\ \boldsymbol{t}\in(-\mathbf{1})^{s}\times[\mathbf{0},\infty)\right\}. \tag{2}$$

For a specified function in the set $\boldsymbol{A}$, the constant $\boldsymbol{M}$ must be a finite value, but $\boldsymbol{\nu}$ may be either finite or infinite.

The Elzaki transform (ET) of $\boldsymbol{\sigma(t)}$ is identified as [52]:

$$\mathfrak{Z}[\sigma(t)](\omega)=T(\omega)=\omega\int_0^{\infty}\exp\left(\frac{-t}{\omega}\right)\sigma(t)dt. \tag{3}$$

Theorem 2.1. The CFET of the CFFD for the function $\boldsymbol{\sigma(t)}$ is identified as [50]:

$$^{CF}\mathfrak{Z}_{\mu}\left\{^{CF}D_t^{\mu}[\sigma(t)]\right\}=\frac{1}{1-\mu+\mu\omega}\left(^{CF}\mathfrak{Z}_{\mu}[\sigma(t)]-\omega^2\sigma(0)\right),0<\mu\leq 1. \tag{4}$$

2.1. The CFq-EHATM

It should be noted that the CFq-EHATM used in this study is adopted from the literature [46]; the novelty of this work lies in its application to the proposed fractional-order drilling model and the analysis of its dynamic behavior.

To elucidate the fundamental concept of CFq-EHATM, I shall analyze the Caputo–Fabrizio partial differential equation (CFPDE):

$$^{CF}D_t^{\mu}\sigma(x,t)+F\sigma(x,t)+R\sigma(x,t)=g(x,t),n-1<\mu\leq n, \tag{5}$$

where *F* shows the linear differential operator, *R* demonstrates the nonlinear differential operator, and g(x,t) is the nonhomogeneous function.

Applying CFET to CFPDE and by utilizing initial condition (IC), it is acquired that

$$\frac{1}{1-\mu+\mu\omega}\left(^{CF}\mathfrak{Z}_{\mu}[\sigma(x,t)]-\omega^2\sigma(x,0)\right)+{}^{CF}\mathfrak{Z}_{\mu}[F\sigma(x,t)+R\sigma(x,t)]={}^{CF}\mathfrak{Z}_{\mu}[g(x,t)]. \tag{6}$$

If I simplify Eq (6), then I get

$$^{CF}\mathfrak{Z}_{\mu}[\sigma(x,t)]-\omega^2\sigma(x,0)+(1-\mu+\mu\omega)^{CF}\mathfrak{Z}_{\mu}[F\sigma(x,t)+R\sigma(x,t)-g(x,t)]=0. \tag{7}$$

Via the help of HAM for $\mathcal{F}(x,t;q)$, the nonlinear operator (NO) is described as [53,54]:

$$\begin{aligned}N[\mathcal{F}(x,t;q)]=&\ ^{CF}\mathfrak{Z}_{\mu}[\mathcal{F}(x,t;q)]-\omega^2\mathcal{F}(x,t;q)(0^{+})+(1-\mu+\mu\omega)\\&\times{}^{CF}\mathfrak{Z}_{\mu}[F\mathcal{F}(x,t;q)+R\mathcal{F}(x,t;q)-g(x,t)],\end{aligned} \tag{8}$$

where $q\epsilon\left[0,\frac{1}{n}\right]$.

A homotopy is constructed as

$$(1-nq)^{CF}\mathfrak{Z}_{\mu}[\mathcal{F}(x,t;q)-\sigma_0(x,t)]=hq\Phi(x,t)N[\mathcal{F}(x,t;q)], \tag{9}$$

where, $n\in\mathbb{N}$ is an auxiliary scaling parameter, and the embedding parameter is defined as $q=1/n$, ensuring that the product nq remains dimensionless and is properly normalized within the homotopy framework. Additionally, $h\neq 0$ and $^{CF}\mathfrak{Z}_{\mu}$ expresses the CFET. For $q=0$ and $q=\frac{1}{n}$, the outcomes are respectively acquired by

$$\mathcal{F}(x,t;0)=\sigma_0(x,t),\mathcal{F}\left(x,t;\frac{1}{n}\right)=\sigma(x,t). \tag{10}$$

Consequently, by increasing q from 0 to 1/n, the solution $\mathcal{F}(x,t;q)$ converges from $\sigma_0(x,t)$ to

the solution $\sigma(x,t)$. Utilizing the Taylor theorem around q and expanding $\mathcal{F}(x,t;q)$, I obtain

$$\mathcal{F}(x,t;q) = \sigma_0(x,t) + \sum_{i=1}^{\infty} \sigma_m(x,t)q^m, \tag{11}$$

where

$$\sigma_m(x,t) = \frac{1}{m!}\frac{\partial^m \mathcal{F}(x,t;q)}{\partial q^m}\Big|_{q=0}. \tag{12}$$

Equation (11) converges at $q = \frac{1}{n}$ for the appropriate $\sigma_0(x,t), n, h$. Therefore, one of the solutions of the nonlinear equation is constructed via

$$\sigma(x,t) = \sigma_0(x,t) + \sum_{m=1}^{\infty} \sigma_m(x,t)\left(\frac{1}{n}\right)^m. \tag{13}$$

Differentiating Eq (9) m-times with regard to q and dividing via $m!$, for $q = 0$, I acquire

$${}^{CF}\mathfrak{Z}_\mu[\sigma_m(x,t) - k_m\sigma_{m-1}(x,t)] = h\Phi(x,t)\mathcal{R}_*(\vec{\sigma}_{m-1}). \tag{14}$$

The inverse CFET is implemented to Eq (14), so I obtain

$$\sigma_m(x,t) = k_m\sigma_{m-1}(x,t) + h\left({}^{CF}\mathfrak{Z}_\mu\right)^{-1}[\Phi(x,t)\mathcal{R}_*(\vec{\sigma}_{m-1})], \tag{15}$$

where

$$\mathcal{R}_*(\vec{\sigma}_{m-1}) = {}^{CF}\mathfrak{Z}_\mu[\sigma_{m-1}(x,t)] - \left(1 - \frac{k_m}{n}\right)(1-\mu+\mu\omega)\sigma_0(x,t)$$
$$+(1-\mu+\mu\omega)\left[{}^{CF}\mathfrak{Z}_\mu[F\sigma_{m-1}(x,t) + \Phi_{m-1}(x,t) - g(x,t)]\right] \tag{16}$$

and

$$k_m = \begin{cases} 0, & m \le 1, \\ n, & m > 1. \end{cases} \tag{17}$$

where Φ_m is homotopy polynomial and it is identified via

$$\Phi_m = \frac{1}{m!}\frac{\partial^m \mathcal{F}(x,t;q)}{\partial q^m}\Big|_{q=0}, \mathcal{F}(x,t;q) = \mathcal{F}_0 + q\mathcal{F}_1 + q^2\mathcal{F}_2 + \cdots. \tag{18}$$

Via Eqs (15) and (16), I get

$$\sigma_m(x,t) = (k_m + h)\sigma_{m-1}(x,t) - \left(1 - \frac{k_m}{n}\right)(1-\mu+\mu\omega)\sigma_0(x,t)$$
$$+h\left({}^{CF}\mathfrak{Z}_\mu\right)^{-1}\left[(1-\mu+\mu\omega)\,{}^{CF}\mathfrak{Z}_\mu\{F\sigma_{m-1}(x,t) + \Phi_{m-1}(x,t) - g(x,t)\}\right]. \tag{19}$$

By using CFq-EHATM, the series solution has the form

$$\sigma(x,t) = \sum_{m=0}^{\infty} \sigma_m(x,t). \tag{20}$$

2.2. Convergence analysis

Theorem 2.2. [55] The solution of CFPDE obtained via CFq-EHATM is unique for $\forall \boldsymbol{\mu} \boldsymbol{\epsilon} (\mathbf{0}, \mathbf{1})$, where $\boldsymbol{\mu} = (\mathbf{n} + \hbar) + \hbar(\boldsymbol{\varphi} + \boldsymbol{\sigma})\boldsymbol{\Omega}$.

Theorem 2.3. [55] Assume that $\boldsymbol{\varrho}$ is Banach space (BS) and $\boldsymbol{\varsigma}: \boldsymbol{\varrho} \to \boldsymbol{\varrho}$ is the nonlinear mapping. The following inequality is provided as

$$\|\rho(\varkappa) - \rho(\kappa)\| \leq \delta\|\varkappa - \kappa\|, \forall \varkappa, \kappa \in \varrho, \tag{21}$$

so $\boldsymbol{\kappa}$ has a fixed point in BS [53]. Furthermore, for any arbitrary selection of $\boldsymbol{\varkappa_0}, \boldsymbol{\kappa_0} \in \boldsymbol{\varrho}$, the sequence acquired via the CFq-EHATM converges to a fixed point of $\boldsymbol{\rho}$ and

$$\|\varkappa_m - \varkappa_n\| \leq \frac{\delta^n}{1-\delta}\|\varkappa_1 - \varkappa_0\|, \forall \varkappa, \kappa \in \varrho. \tag{22}$$

3. The analysis of mathematical modeling for the drilling system

Before introducing the fractional order formulation, the corresponding full order drilling system model can be expressed in the classical form given in [54] by Eq (23). This formulation describes the combined electromechanical dynamics of the drilling system without memory effects.

3.1. The analysis of classical mathematical modeling for the drilling system

$$\begin{aligned}
\frac{dA(\tau)}{d\tau} &= C(\tau)M(\tau) - \lambda_1 A(\tau),\\
\frac{dC(\tau)}{d\tau} &= -\lambda_1 C(\tau) - M(\tau) - A(\tau)M(\tau),\\
\frac{dH(\tau)}{d\tau} &= \lambda_1 H(\tau),\\
\frac{dL(\tau)}{d\tau} &= V(\tau) - M(\tau),\\
\frac{dM(\tau)}{d\tau} &= \lambda_2 L(\tau) + \lambda_3\big(V(\tau) - M(\tau)\big) + \lambda_4 C(\tau),\\
\frac{dV(\tau)}{d\tau} &= \lambda_5 L(\tau) + \lambda_6\big(V(\tau) - M(\tau)\big) + \lambda_7\big(\varpi - V(\tau)\big).
\end{aligned} \tag{23}$$

The fractional-order model presented in Eq (23) is obtained by generalizing the integer-order system through the use of the Caputo–Fabrizio fractional derivative of order $\mu \in (0,1]$. This formulation enables the incorporation of memory effects associated with frictional interaction, distributed damping, and delayed energy transfer along the drill string.

3.2. The analysis of Caputo–Fabrizio fractional mathematical modeling for the drilling system

Fractional-order systems can also be grouped either as commensurate or incommensurate, depending on whether the orders of derivatives are the same or different. In commensurate systems, all fractional derivatives follow the same order, which eases the analytical formulation and numerical implementation. Incommensurate systems, in contrast, involve derivatives of different orders, leading to more complex dynamics and analysis. Thus, system (24), which is a commensurate fractional-order system, is presented in this study because it enables a definition of all derivative terms in the same fractional order μ, so that a consistent and manageable framework can be created.

Although fractional-order models of drilling systems have been studied, the current approach uses the non-singular exponential kernel of the Caputo–Fabrizio fractional derivative, which enables smoother memory behavior and eliminates singularities inherent in classical formulations. It is

particularly suitable for representing gradual energy dissipation and fading memory effects observed in drilling dynamics. It also has a simple analytical structure, which makes it an efficient implementation of the proposed semi-analytical method.

The CFFMMDS actuated by an induction motor is analyzed as follows [49]:

$$
\begin{aligned}
{}^{CF}D_{\tau}^{\mu}A(\tau) &= C(\tau)M(\tau) - \lambda_1 A(\tau),\\
{}^{CF}D_{\tau}^{\mu}C(\tau) &= -\lambda_1 C(\tau) - M(\tau) - A(\tau)M(\tau),\\
{}^{CF}D_{\tau}^{\mu}H(\tau) &= \lambda_1 H(\tau),\\
{}^{CF}D_{\tau}^{\mu}L(\tau) &= V(\tau) - M(\tau),\\
{}^{CF}D_{\tau}^{\mu}M(\tau) &= \lambda_2 L(\tau) + \lambda_3\big(V(\tau) - M(\tau)\big) + \lambda_4 C(\tau),\\
{}^{CF}D_{\tau}^{\mu}V(\tau) &= \lambda_5 L(\tau) + \lambda_6\big(V(\tau) - M(\tau)\big) + \lambda_7\big(\varpi - V(\tau)\big),
\end{aligned}
\tag{24}
$$

subject to ICs $\boldsymbol{A(0) = 0.09, C(0) = -0.09, H(0) = -0.9, L(0) = -0.1, M(0) = 0.2, V(0) = -0.3}$, where $\boldsymbol{\mu \in (0,1]}$ is the order of fractional derivative. $\boldsymbol{A(\tau)}$ depicts the torsional state on the motor/upper disk side, $\boldsymbol{C(\tau)}$ the torsional state on the load/lower disk (bit side), $\boldsymbol{H(\tau)}$ the electrical–electromechanical state on the motor side, $\boldsymbol{L(\tau)}$ the relative angular difference (torsional twist) between the motor and load sides, $\boldsymbol{M(\tau)}$ the friction/resistance state caused by bit-rock contact, and $\boldsymbol{V(\tau)}$ the motor-side speed/electromechanical state corresponding to the induction motor's tendency toward nominal angular velocity [54].

Fractional ordering systems can be of two kinds, commensurate or incommensurate, based on whether all the state equations share the same derivative order or involve different orders. In this work, system (24) is presented as a commensurate fractional-order system since all derivatives are taken with the same order μ. This decision is taken to maintain a constant structure of the memory for all state variables and facilitates the construction of the CFq-EHATM approach to achieve greater interpretability in the effect of μ on the system dynamics as a whole. In contrast, incommensurate systems tend to have richer but more mathematically demanding behavior, and work has been concerned with their well-posedness and solution structure in delay and continuous-function settings. Moreover, the incommensurate delay fractional differential systems and incommensurate FDEs in spaces of continuous functions have also demonstrated improved theoretical interest in these type of systems [56,57].

Since the governing equations are expressed in a dimensionless framework, the use of fractional derivatives does not violate dimensional consistency while acting on normalized state variables and preserving the physical structure of the system.

These initial conditions in the above-mentioned work are generally taken as being analogous to the normalized drilling system setting reported in [54]. These values are not precise experimental results but rather representative dimensionless initial states chosen to examine the transient response of the coupled system under a perturbed operating configuration.

Table 1 shows the parameter definitions and values used for CFFMMDS.

Table 1. Descriptions of the model parameters [54].

Parameter	Description	Value
λ_1	Electrical damping coefficient of the induction motor, representing the ratio of resistance to inductance	0.06
λ_2	Normalized torsional stiffness coefficient acting on the upper disk (motor side), relative to its inertia	0.157
λ_3	Normalized viscous damping coefficient associated with the upper disk dynamics	0.018
λ_4	Normalized electromagnetic coupling coefficient reflecting the influence of motor current on the upper disk	4.407
λ_5	Normalized torsional stiffness coefficient acting on the lower disk (load side)	2.142
λ_6	Normalized viscous damping coefficient associated with the lower disk dynamics	0.257
λ_7	Normalized friction torque coefficient acting on the lower disk	7.428
ϖ	Nominal angular velocity of the induction motor	6

The parameter values for Table 1 are chosen within physically reasonable ranges and in line with reported values for similar drilling system models. These are selected to guarantee realistic behavior and make it easier to investigate the role of fractional order μ.

Applying CFET to Eq (24) and by utilizing ICs, it is acquired that

$$ {}^{CF}\mathfrak{Z}_\mu[A(\tau)] - \omega^2 A(0) - (1-\mu+\mu\omega)\,{}^{CF}\mathfrak{Z}_\mu[C(\tau)M(\tau) - \lambda_1 A(\tau)] = 0, \tag{25} $$

$$ {}^{CF}\mathfrak{Z}_\mu[C(\tau)] - \omega^2 C(0) - (1-\mu+\mu\omega)\,{}^{CF}\mathfrak{Z}_\mu[-\lambda_1 C(\tau) - M(\tau) - A(\tau)M(\tau)] = 0, \tag{26} $$

$$ {}^{CF}\mathfrak{Z}_\mu[H(\tau)] - \omega^2 H(0) - (1-\mu+\mu\omega)\,{}^{CF}\mathfrak{Z}_\mu[\lambda_1 H(\tau)] = 0, \tag{27} $$

$$ {}^{CF}\mathfrak{Z}_\mu[L(\tau)] - \omega^2 L(0) - (1-\mu+\mu\omega)\,{}^{CF}\mathfrak{Z}_\mu[V(\tau) - M(\tau)] = 0, \tag{28} $$

$$ {}^{CF}\mathfrak{Z}_\mu[M(\tau)] - \omega^2 M(0) - (1-\mu+\mu\omega)\,{}^{CF}\mathfrak{Z}_\mu\big[\lambda_2 L(\tau) + \lambda_3\big(V(\tau) - M(\tau)\big) + \lambda_4 C(\tau)\big] = 0, \tag{29} $$

$$ {}^{CF}\mathfrak{Z}_\mu[V(\tau)] - \omega^2 V(0) - (1-\mu+\mu\omega)\,{}^{CF}\mathfrak{Z}_\mu\big[\lambda_5 L(\tau) + \lambda_6\big(V(\tau) - M(\tau)\big) + \lambda_7\big(\varpi - V(\tau)\big)\big] = 0. \tag{30} $$

The nonlinear operators $\varphi_1, \varphi_2, \varphi_3, \varphi_4, \varphi_5, \varphi_6$ are defined by

$$ N_1[\varphi_1(\tau;q);\varphi_2(\tau;q);\varphi_3(\tau;q);\varphi_4(\tau;q);\varphi_5(\tau;q);\varphi_6(\tau;q)] $$
$$ = {}^{CF}\mathfrak{Z}_\mu[\varphi_2(\tau;q)] + 0.09\omega^2 - (1-\mu+\mu\omega)\,{}^{CF}\mathfrak{Z}_\mu[\varphi_2(\tau;q)\varphi_5(\tau;q) - \lambda_1\varphi_1(\tau;q)], \tag{31} $$

$$ N_2[\varphi_1(\tau;q);\varphi_2(\tau;q);\varphi_3(\tau;q);\varphi_4(\tau;q);\varphi_5(\tau;q);\varphi_6(\tau;q)] $$
$$ = {}^{CF}\mathfrak{Z}_\mu[\varphi_2(\tau;q)] + 0.09\omega^2 - (1-\mu+\mu\omega)\,{}^{CF}\mathfrak{Z}_\mu[-\lambda_1\varphi_2(\tau;q) - \varphi_5(\tau;q) - \varphi_1(\tau;q)\varphi_5(\tau;q)], \tag{32} $$

$$ N_3[\varphi_1(\tau;q);\varphi_2(\tau;q);\varphi_3(\tau;q);\varphi_4(\tau;q);\varphi_5(\tau;q);\varphi_6(\tau;q)] $$
$$ = {}^{CF}\mathfrak{Z}_\mu[\varphi_3(\tau;q)] + 0.9\omega^2 - (1-\mu+\mu\omega)\,{}^{CF}\mathfrak{Z}_\mu[\lambda_1\varphi_3(\tau;q)], \tag{33} $$

$$ N_4[\varphi_1(\tau;q);\varphi_2(\tau;q);\varphi_3(\tau;q);\varphi_4(\tau;q);\varphi_5(\tau;q);\varphi_6(\tau;q)] $$
$$ = {}^{CF}\mathfrak{Z}_\mu[\varphi_4(\tau;q)] + 0.1\omega^2 - (1-\mu+\mu\omega)\,{}^{CF}\mathfrak{Z}_\mu[\varphi_6(\tau;q) - \varphi_5(\tau;q)], \tag{34} $$

$$ N_5[\varphi_1(\tau;q);\varphi_2(\tau;q);\varphi_3(\tau;q);\varphi_4(\tau;q);\varphi_5(\tau;q);\varphi_6(\tau;q)] = {}^{CF}\mathfrak{Z}_\mu[\varphi_5(\tau;q)] - 0.2\omega^2 $$
$$ -(1-\mu+\mu\omega)\,{}^{CF}\mathfrak{Z}_\mu\big[\lambda_2\varphi_4(\tau;q) + \lambda_3\big(\varphi_6(\tau;q) - \varphi_5(\tau;q)\big) + \lambda_4\varphi_2(\tau;q)\big], \tag{35} $$

$$N_6[\varphi_1(\tau;q);\varphi_2(\tau;q);\varphi_3(\tau;q);\varphi_4(\tau;q);\varphi_5(\tau;q);\varphi_6(\tau;q)] = {}^{CF}\mathfrak{Z}_\mu[\varphi_6(\tau;q)] + 0.3\omega^2$$
$$-(1-\mu+\mu\omega)\,{}^{CF}\mathfrak{Z}_\mu\big[\lambda_5\varphi_4(\tau;q) + \lambda_6\big(\varphi_6(\tau;q) - \varphi_5(\tau;q)\big) + \lambda_7\big(\varpi - \varphi_6(\tau;q)\big)\big]. \tag{36}$$

Therefore, the m-th order deformation equations are given as

$${}^{CF}\mathfrak{Z}_\mu[A_m(\tau) - k_m A_{m-1}(\tau)] = h\mathfrak{R}_{1,*}\big[\big(\vec{A}_{\mathrm{m}-1}, \vec{C}_{\mathrm{m}-1}, \vec{H}_{\mathrm{m}-1}, \vec{L}_{\mathrm{m}-1}, \vec{M}_{\mathrm{m}-1}, \vec{V}_{\mathrm{m}-1}\big)\big], \tag{37}$$

$${}^{CF}\mathfrak{Z}_\mu[C_m(\tau) - k_m C_{m-1}(\tau)] = h\mathfrak{R}_{2,*}\big[\big(\vec{A}_{m-1}, \vec{C}_{m-1}, \vec{H}_{m-1}, \vec{L}_{m-1}, \vec{M}_{m-1}, \vec{V}_{m-1}\big)\big], \tag{38}$$

$${}^{CF}\mathfrak{Z}_\mu[H_m(\tau) - k_m H_{m-1}(\tau)] = h\mathfrak{R}_{3,*}\big[\big(\vec{A}_{m-1}, \vec{C}_{m-1}, \vec{H}_{m-1}, \vec{L}_{m-1}, \vec{M}_{m-1}, \vec{V}_{m-1}\big)\big], \tag{39}$$

$${}^{CF}\mathfrak{Z}_\mu[L_m(\tau) - k_m L_{m-1}(\tau)] = h\mathfrak{R}_{4,*}\big[\big(\vec{A}_{m-1}, \vec{C}_{m-1}, \vec{H}_{m-1}, \vec{L}_{m-1}, \vec{M}_{m-1}, \vec{V}_{m-1}\big)\big], \tag{40}$$

$${}^{CF}\mathfrak{Z}_\mu[M_m(\tau) - k_m M_{m-1}(\tau)] = h\mathfrak{R}_{5,*}\big[\big(\vec{A}_{m-1}, \vec{C}_{m-1}, \vec{H}_{m-1}, \vec{L}_{m-1}, \vec{M}_{m-1}, \vec{V}_{m-1}\big)\big], \tag{41}$$

$${}^{CF}\mathfrak{Z}_\mu[V_m(\tau) - k_m V_{m-1}(\tau)] = h\mathfrak{R}_{6,*}\big[\big(\vec{A}_{m-1}, \vec{C}_{m-1}, \vec{H}_{m-1}, \vec{L}_{m-1}, \vec{M}_{m-1}, \vec{V}_{m-1}\big)\big], \tag{42}$$

where

$$\mathfrak{R}_{1,*}\big[\big(\vec{A}_{m-1}, \vec{C}_{m-1}, \vec{H}_{m-1}, \vec{L}_{m-1}, \vec{M}_{m-1}, \vec{V}_{m-1}\big)\big] = {}^{CF}\mathfrak{Z}_\mu[A_{m-1}(\tau;q)] - 0.09\omega^2\left(1 - \frac{k_m}{n}\right)$$
$$-(1-\mu+\mu\omega)\,{}^{CF}\mathfrak{Z}_\mu\big[\textstyle\sum_{s=0}^{m-1} C_s\, M_{m-1-s} - \lambda_1 A_{m-1}\big], \tag{43}$$

$$\mathfrak{R}_{2,*}\big[\big(\vec{A}_{m-1}, \vec{C}_{m-1}, \vec{H}_{m-1}, \vec{L}_{m-1}, \vec{M}_{m-1}, \vec{V}_{m-1}\big)\big] = {}^{CF}\mathfrak{Z}_\mu[C_{m-1}(\tau;q)] + 0.09\omega^2\left(1 - \frac{k_m}{n}\right)$$
$$-(1-\mu+\mu\omega)\,{}^{CF}\mathfrak{Z}_\mu\big[-\lambda_1 C_{m-1} - M_{m-1} - \textstyle\sum_{s=0}^{m-1} A_s\, M_{m-1-s}\big], \tag{44}$$

$$\mathfrak{R}_{3,*}\big[\big(\vec{A}_{m-1}, \vec{C}_{m-1}, \vec{H}_{m-1}, \vec{L}_{m-1}, \vec{M}_{m-1}, \vec{V}_{m-1}\big)\big] = {}^{CF}\mathfrak{Z}_\mu[H_{m-1}(\tau;q)] + 0.9\omega^2\left(1 - \frac{k_m}{n}\right)$$
$$-(1-\mu+\mu\omega)\,{}^{CF}\mathfrak{Z}_\mu[\lambda_1 H_{m-1}], \tag{45}$$

$$\mathfrak{R}_{4,*}\big[\big(\vec{A}_{m-1}, \vec{C}_{m-1}, \vec{H}_{m-1}, \vec{L}_{m-1}, \vec{M}_{m-1}, \vec{V}_{m-1}\big)\big] = {}^{CF}\mathfrak{Z}_\mu[L_{m-1}(\tau;q)] + 0.1\omega^2\left(1 - \frac{k_m}{n}\right)$$
$$-(1-\mu+\mu\omega)\,{}^{CF}\mathfrak{Z}_\mu[V_{m-1} - M_{m-1}], \tag{46}$$

$$\mathfrak{R}_{5,*}\big[\big(\vec{A}_{m-1}, \vec{C}_{m-1}, \vec{H}_{m-1}, \vec{L}_{m-1}, \vec{M}_{m-1}, \vec{V}_{m-1}\big)\big] = {}^{CF}\mathfrak{Z}_\mu[M_{m-1}(\tau;q)] - 0.2\omega^2\left(1 - \frac{k_m}{n}\right)$$
$$-(1-\mu+\mu\omega)\,{}^{CF}\mathfrak{Z}_\mu[\lambda_2 L_{m-1} + \lambda_3(V_{m-1} - M_{m-1}) + \lambda_4 C_{m-1}], \tag{47}$$

$$\mathfrak{R}_{6,*}\big[\big(\vec{A}_{m-1}, \vec{C}_{m-1}, \vec{H}_{m-1}, \vec{L}_{m-1}, \vec{M}_{m-1}, \vec{V}_{m-1}\big)\big] = {}^{CF}\mathfrak{Z}_\mu[V_{m-1}(\tau;q)] + 0.3\omega^2\left(1 - \frac{k_m}{n}\right)$$
$$-(1-\mu+\mu\omega)\,{}^{CF}\mathfrak{Z}_\mu[\lambda_5 L_{m-1} + \lambda_6(V_{m-1} - M_{m-1}) + \lambda_7(\varpi - V_{m-1})]. \tag{48}$$

On applying inverse CFET on Eqs (37)–(42), it is acquired that

$$A_m(\tau) = k_m A_{m-1}(\tau) + h\big({}^{CF}\mathfrak{Z}_\mu\big)^{-1}\Big[\mathfrak{R}_{1,*}\big[\big(\vec{A}_{m-1}, \vec{C}_{m-1}, \vec{H}_{m-1}, \vec{L}_{m-1}, \vec{M}_{m-1}, \vec{V}_{m-1}\big)\big]\Big], \tag{49}$$

$$C_m(\tau) = k_m C_{m-1}(\tau) + \hbar\big({}^{CF}\mathfrak{Z}_\mu\big)^{-1}\Big[\mathfrak{R}_{2,*}\big[\big(\vec{A}_{m-1}, \vec{C}_{m-1}, \vec{H}_{m-1}, \vec{L}_{m-1}, \vec{M}_{m-1}, \vec{V}_{m-1}\big)\big]\Big], \tag{50}$$

$$H_m(\tau) = k_m H_{m-1}(\tau) + \hbar\left({}^{CF}\mathfrak{Z}_\mu\right)^{-1}\left[\Re_{3,*}\left[\left(\vec{A}_{m-1}, \vec{C}_{m-1}, \vec{H}_{m-1}, \vec{L}_{m-1}, \vec{M}_{m-1}, \vec{V}_{m-1}\right)\right]\right], \quad (51)$$

$$L_m(\tau) = k_m L_{m-1}(\tau) + \hbar\left({}^{CF}\mathfrak{Z}_\mu\right)^{-1}\left[\Re_{4,*}\left[\left(\vec{A}_{m-1}, \vec{C}_{m-1}, \vec{H}_{m-1}, \vec{L}_{m-1}, \vec{M}_{m-1}, \vec{V}_{m-1}\right)\right]\right], \quad (52)$$

$$M_m(\tau) = k_m M_{m-1}(\tau) + \hbar\left({}^{CF}\mathfrak{Z}_\mu\right)^{-1}\left[\Re_{5,*}\left[\left(\vec{A}_{m-1}, \vec{C}_{m-1}, \vec{H}_{m-1}, \vec{L}_{m-1}, \vec{M}_{m-1}, \vec{V}_{m-1}\right)\right]\right], \quad (53)$$

$$V_m(\tau) = k_m V_{m-1}(\tau) + \hbar\left({}^{CF}\mathfrak{Z}_\mu\right)^{-1}\left[\Re_{6,*}\left[\left(\vec{A}_{m-1}, \vec{C}_{m-1}, \vec{H}_{m-1}, \vec{L}_{m-1}, \vec{M}_{m-1}, \vec{V}_{m-1}\right)\right]\right]. \quad (54)$$

By applying the iterative scheme defined in Eqs (49)–(54) for $m = 0,1,2,\ldots$, the first few components of the solution series are obtained as follows: Using the ICs, I have

$$A_0(\tau) = 0.09, C_0(\tau) = -0.09, H_0(\tau) = -0.9, L_0(\tau) = -0.1, M_0(\tau) = 0.2, V_0(\tau) = -0.3. \quad (55)$$

To ascertain the values of $A_1(\tau), C_1(\tau), H_1(\tau), L_1(\tau), M_1(\tau), V_1(\tau)$, replace $m = 1$ into Eqs (49)–(54), accordingly, yielding

$$A_1(\tau) = -h(1-\mu+\mu\tau)(-0.09\lambda_1 - 0.018), \quad (56)$$

$$C_1(\tau) = -h(1-\mu+\mu\tau)(0.09\lambda_1 - 0.218), \quad (57)$$

$$H_1(\tau) = h(1-\mu+\mu\tau)(0.9\lambda_1), \quad (58)$$

$$L_1(\tau) = 0.5h(1-\mu+\mu\tau), \quad (59)$$

$$M_1(\tau) = -h(1-\mu+\mu\tau)(-0.1\lambda_2 - 0.5\lambda_3 - 0.09\lambda_4), \quad (60)$$

$$V_1(\tau) = -h(1-\mu+\mu\tau)(-0.1\lambda_5 - 0.5\lambda_6 + \lambda_7(\varpi + 0.3)). \quad (61)$$

It should be noted that the numerical coefficients appearing in this expression are obtained by direct substitution of the parameter values listed in Table 1 into the analytical formulation and do not represent additional independent parameters.

Similarly, to ascertain the values of $A_2(\tau), C_2(\tau), H_2(\tau), L_2(\tau), M_2(\tau), V_2(\tau)$, putting $m = 2$ into Eqs (49)–(54) yields

$$A_2(\tau) = (n+h)[-h(1-\mu+\mu\tau)(-0.09\lambda_1 - 0.018)]$$
$$+h^2\psi(\mu,\tau)\left(0.09{\lambda_1}^2 + 0.036\lambda_1 + 0.009\lambda_2 + 0.045\lambda_3 + 0.0081\lambda_4 - 0.0436\right), \quad (62)$$

$$C_2(\tau) = (n+h)[-h(1-\mu+\mu\tau)(0.09\lambda_1 - 0.218)] - h^2\psi(\mu,\tau)$$
$$\times(-0.109\lambda_2 - 0.545\lambda_3 - 0.0981\lambda_4 - 0.236\lambda_1 - 0.0036 + 0.09{\lambda_1}^2), \quad (63)$$

$$H_2(\tau) = (n+h)[h(1-\mu+\mu\tau)(0.9\lambda_1)] - 0.9h^2{\lambda_1}^2\psi(\mu,\tau), \quad (64)$$

$$L_2(\tau) = (n+h)[0.5h(1-\mu+\mu\tau)] + h^2\psi(\mu,\tau)(\lambda_7(\varpi+0.3) - 0.1\lambda_5$$
$$-0.5\lambda_6 + 0.1\lambda_2 + 0.5\lambda_3 + 0.09\lambda_4), \quad (65)$$

$$M_2(\tau) = (n+h)[-h(1-\mu+\mu\tau)(-0.1\lambda_2 - 0.5\lambda_3 - 0.09\lambda_4)]$$
$$-h\psi(\mu,\tau)(0.5\lambda_2 h\psi(\mu,\tau) - h(\lambda_7(\varpi+0.3) - 0.1\lambda_5 - 0.5\lambda_6$$
$$+0.1\lambda_2 + 0.5\lambda_3 + 0.09\lambda_4)\psi(\mu,\tau)\lambda_3 - \lambda_4 h\psi(\mu,\tau)(0.09\lambda_1 - 0.218)), \quad (66)$$

$$V_2(\tau) = (n+h)[-h(1-\mu+\mu\tau)(-0.1\lambda_5 - 0.5\lambda_6 + \lambda_7(\varpi+0.3))]$$

$$-h\psi(\mu,\tau)(0.5\lambda_5 h-\lambda_6 h(\lambda_7(\varpi+0.3)-0.1\lambda_5-0.5\lambda_6+0.1\lambda_2+0.5\lambda_3$$
$$+0.09\lambda_4)+\big((h(\tau-1)\lambda_7\varpi+(0.3\tau-0.3)h\lambda_7+\big((-0.1\lambda_5-0.5\lambda_6\big)\tau+0.1\lambda_5$$
$$+0.5\lambda_6)h)\mu+(h\lambda_7+1)\varpi+0.3h\lambda_7+(-0.1\lambda_5-0.5\lambda_6)h)\lambda_7), \quad (67)$$
$$\vdots$$

In Eqs (62)–(67),

$$\psi(\mu,\tau)=\left((1-\mu)^2+2\mu(1-\mu)t+\frac{\mu^2t^2}{2}\right)$$

is given as the expression. Additionally, $\psi(\mu,\tau)$ is obtained from the analytical formulation of the Caputo–Fabrizio fractional derivative after algebraic simplification and does not represent an assumed series approximation.

Higher-order terms become more complex as the series converges quickly and contribute only marginally to the solution accuracy. Therefore, only the first few terms are given, which are enough to represent the fundamental behavior of the system. Thus, the CFq-EHATM solutions of CFFMMDS are introduced by

$$A(\tau)=A_0(\tau)+\sum_{m=1}^{\infty}A_m(\tau), \quad (68)$$
$$C(\tau)=C_0(\tau)+\sum_{m=1}^{\infty}C_m(\tau), \quad (69)$$
$$H(\tau)=H_0(\tau)+\sum_{m=1}^{\infty}H_m(\tau), \quad (70)$$
$$L(\tau)=L_0(\tau)+\sum_{m=1}^{\infty}L_m(\tau), \quad (71)$$
$$M(\tau)=M_0(\tau)+\sum_{m=1}^{\infty}M_m(\tau), \quad (72)$$
$$V(\tau)=V_0(\tau)+\sum_{m=1}^{\infty}V_m(\tau). \quad (73)$$

4. Results and discussion

The truncated series representation is sufficient due to its rapid convergence. Numerical results are presented to analyze the system response under varying fractional orders using the Caputo–Fabrizio fractional derivative. In the following figures, two-dimensional solution profiles of the CFFMMDS are plotted for $h=-1$, $n=1$, and different values of μ, based on the parameter set reported in Table 1.

In Figure 2, the temporal evolution of $A(\tau)$ is presented, while all other model parameters are fixed, as given in Table 1. The curves illustrate that decreasing μ leads to a reduction in the magnitude of growth and decay slopes. In Figure 3, the results demonstrate that lower values of μ yield a smoother temporal response, indicating enhanced memory effects within the system. In Figure 4, as the fractional order decreases, the evolution of $H(\tau)$ becomes more gradual, reflecting attenuation in the dynamic response. The Figure 5 shows that decreasing μ reduces the rate of change in $L(\tau)$, leading to a smoother and more distributed temporal behavior. In Figure 6, a damping-like effect is observed as μ decreases, resulting in reduced slope magnitudes. In Figure 7, the results indicate that smaller values of μ produce a slower and smoother temporal evolution, which is consistent with the memory-dependent nature of the fractional operator.

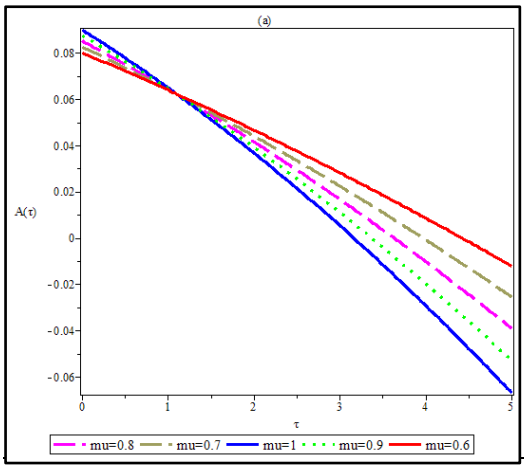

Figure 2. Two-dimensional plot of solution $A(\tau)$ obtained via the CFFMMDS for different values of the fractional-order parameter μ.

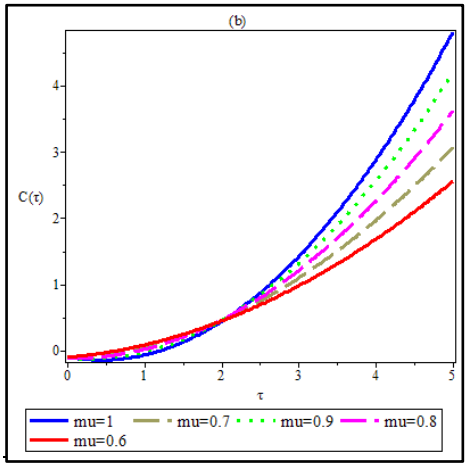

Figure 3. Two-dimensional plot of solution $C(\tau)$ for varying fractional-order values μ.

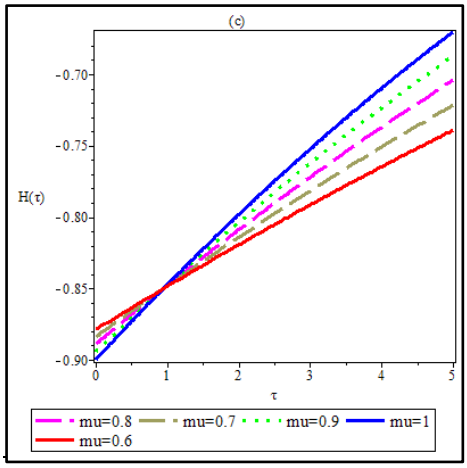

Figure 4. Two-dimensional plot of solution $H(\tau)$ under different values of μ.

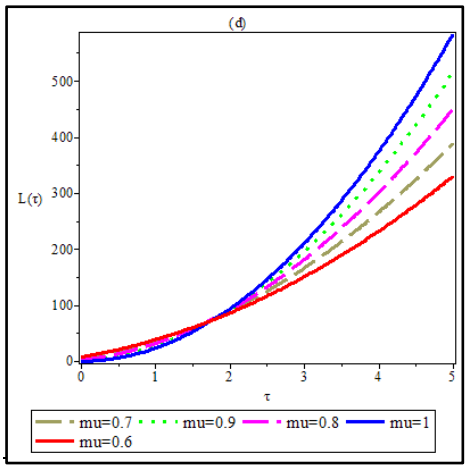

Figure 5. Two-dimensional plot of solution $L(\tau)$ for varying μ.

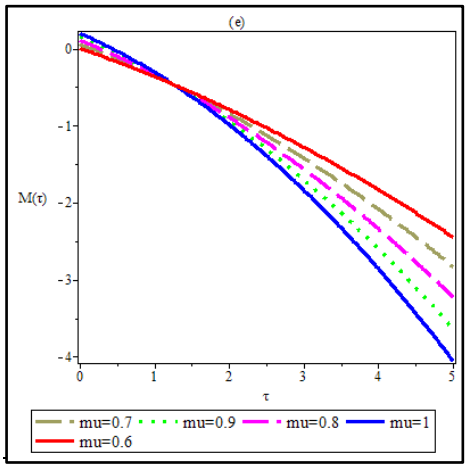

Figure 6. Two-dimensional plot of the solution $M(\tau)$ corresponding to different fractional orders μ.

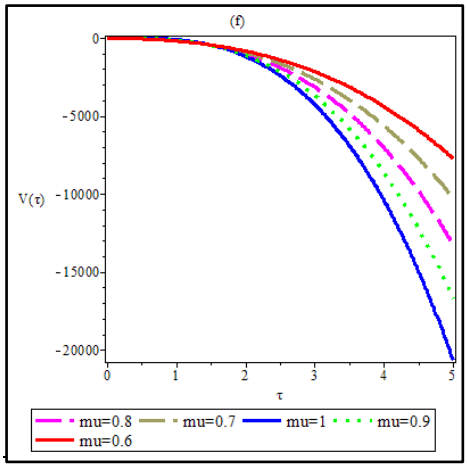

Figure 7. Two-dimensional plot of the solution $V(\tau)$ for different values of μ.

For example, the fractional order can be illustrated further by studying the solutions concerning different μ of solutions. I find that a decreasing μ results in a slower evolving time scale with a

smoother system reaction that seems to have stronger memory effects. The magnitude of values μ close to 1, by contrast, reproduces behavior resembling the classical integer-order model. These numerical effects validate the large importance of the fractional order in determining the dynamic properties of the system and its stability.

These results can be understood in terms of the physical behavior of the drilling system. Moreover, decreasing fractional order μ introduces stronger memory effects, which act as a damping-like mechanism in the system. As a result, the amplitude of oscillations decreases accordingly, and the temporal response becomes smoother. This behavior, from a drilling engineering perspective, is related to the suppression of undesirable vibration phenomena, including stick-slip oscillations and fluctuations in torque and angular velocity. In addition, the attenuation indicates enhanced energy dissipation within the system, which contributes to improved operational stability and reduced mechanical stress on drilling components.

In this study, a strict stability or bifurcation analysis is not performed, but the results give qualitative information about system dynamics. In particular, decreasing fractional order μ leads to smoother responses of the system and reduced oscillation amplitudes, suggesting enhanced stability due to stronger memory effects. A detailed stability and bifurcation analysis of the proposed fractional-order model constitutes an interesting direction for future work.

The time-dependent decay rate of $A(\tau)$ is strongly dependent on fractional order μ. As μ decreases, the magnitude of the slope of $A(\tau)$ is reduced, and the temporal evolution of the solution becomes slower and more gradual compared to the integer-order case. Similarly, the time-dependent growth behavior of $C(\tau)$ exhibits smaller growth slopes for decreasing values of μ, leading to a more gradual progression of the solution over time. For $H(\tau)$, a comparable trend is observed, where a decrease in μ results in a reduced magnitude of the decay slope and a slower temporal evolution. As shown in Figure 5, the growth rate of $L(\tau)$ is also sensitive to the fractional order, with lower values of μ yielding diminished growth slopes and a more gradual development of the solution. This tendency is further reflected in Figure 6 by the decreasing magnitude of the negative slope of $M(\tau)$, and in Figure 7 by the more gradual temporal variation of $V(\tau)$. Overall, the results presented in Figures 2–7 indicate that a decrease in fractional order μ systematically attenuates growth and decay slopes across all state variables, leading to a slower and more distributed temporal evolution relative to the classical integer-order formulation. With decreasing fractional order μ, there is attenuation of growth and decay slopes, and this can physically be interpreted as a result of enhanced memory effects in the system. In contrast to classical integer-order models, this fractional representation works in a way that incorporates past states into the current processes, which leads to smoothing out the temporal evolution over time. The damping-like effect of this phenomenon could be attributed from the drilling engineering standpoint. In particular, the lower rate of change in the state variables suggests a suppression of rapid oscillations, such as stick-slip vibrations that are common in drilling systems. Consequently, lower values of μ may correspond to improved dynamic stability, reduced mechanical wear, and more efficient drilling performance. This unified trend reflects the intrinsic memory structure of the Caputo–Fabrizio fractional derivative, which distributes the influence of past states over the temporal domain of the solution space.

The semi-analytical solutions obtained provide a better appreciation of the dynamic response of the drilling system to fractional-order effects. More specifically, they enable investigation of how fundamental parameters and the fractional order μ contribute to system stability, transient behavior, and oscillatory patterns. In a practical sense, this may contribute to better vibration phenomena control, i.e., stick-slip oscillations, and better understanding of energy dissipation mechanisms in drilling. In addition, because the solution can be used as an analytical form, efficient parametric studies make the

results of the analysis of the solution for optimization and design of more stable and reliable drilling operations feasible.

5. Conclusions

My goal of this study was to develop a CFFMMDS mathematical model to investigate the dynamics of the components of an induction motor-driven drilling system. To examine the influence of the fractional order μ on the temporal behavior of the system state variables, a nonsingular fractional derivative with an exponential memory kernel was incorporated into the governing equations. The results show that decreasing μ yields smaller growth and decay slopes, indicating a slower and more gradual temporal evolution compared to the classical integer-order formulation. This trend is consistent with the memory structure of the Caputo–Fabrizio operator, which distributes the influence of past states over time. Overall, the most important contributions of this study can be emphasized as follows: First, a fractional-order model of the drilling system is developed using the Caputo–Fabrizio derivative, which can integrate the non-singular memory effects. Second, a hybrid semi-analytical approach based on the CFq-EHATM method is employed to generate approximate solution series for the proposed system. Third, the effect of fractional order μ on the system dynamics is systematically evaluated, proving its key involvement in controlling stability and transient behavior. Finally, the results obtained provide useful insights into vibration attenuation and energy dissipation mechanisms, thus contributing to a better understanding of drilling system dynamics. Despite the excellent results of this study, there are some limitations that must be mentioned. The model proposed is of a commensurate fractional-order formulation and it takes a simplified characterization of the dynamics of the drilling system. Additionally, the semi-analytical CFq-EHATM solutions are presented as truncated versions, and higher-order terms are not specified because they become more complex. Moreover, researchers could expand the approach to incommensurate fractional-order systems, incorporate more realistic physical effects, and validate the results with experimental or field data. It has also been suggested that efficient numerical schemes will be used for numerical modeling, so hybrid approaches toward more complex fractional models must remain a good direction for future research. It should be noted that my results primarily illustrate qualitative trends of the system behavior. A quantitative validation with experimental or benchmark data remains an important direction for future research. A detailed comparison with numerical methods such as the finite difference method is left for future work and will be addressed in subsequent studies.

Use of Generative-AI tools declaration

The author declares he has not used Artificial Intelligence (AI) tools in the creation of this article.

Conflict of interest

The author declares there is no conflict of interest.

References

1. M. Z. Doghmane, Nonlinear dynamic modeling and analysis of drill strings under stick-slip vibrations in rotary drilling systems, *Energies*, **18** (2025), 3860. https://doi.org/10.3390/en18143860

2. M. J. Moharrami, H. Shiri, C. de A. Martins, Numerical investigation of the nonlinear drill string dynamics under stick-slip vibration, *Vibration*, **7** (2024), 1086–1110. https://doi.org/10.3390/vibration7040056
3. A. Ghasemloonia, D. G. Rideout, S. D. Butt, A review of drillstring vibration modeling and suppression methods, *J. Pet. Sci. Eng.*, **131** (2015), 150–164. http://dx.doi.org/10.1016/j.petrol.2015.04.030
4. E. Detournay, P. Defourny, A phenomenological model for the drilling action of drag bits, *Int. J. Rock Mech. Min. Sci. Geomech. Abstracts*, **29** (1992), 13–23. https://doi.org/10.1016/0148-9062(92)91041-3
5. A. Guzek, I. Shufrin, E. Pasternak, A. V. Dyskin, Influence of drilling mud rheology on the reduction of vertical vibrations in deep rotary drilling, *J. Pet. Sci. Eng.*, **135** (2015), 375–383. https://doi.org/10.1016/j.petrol.2015.09.016
6. M. Zamanian, S. E. Khadem, M. R. Ghazavi, Stick-slip oscillations of drag bits by considering damping of drilling mud and active damping system, *J. Pet. Sci. Eng.*, **59** (2007), 289–299. https://doi.org/10.1016/j.petrol.2007.04.008
7. O. Allain, M. Dyson, X. Jing, C. Pentland, M. Polikar, V. S. Suicmez, *Drilling and reservoir appraisal*, World Scientific, 2019.
8. J. D. Jansen, *Nonlinear dynamics of oilwell drillstrings*, Ph. D. Thesis, Delft University of Technology, 1993.
9. J. F. Brett, The genesis of torsional drillstring vibrations, *SPE Drill. Eng.*, **7** (1992), 168–172. https://doi.org/10.2118/21944-PA
10. D. R. Pavone, J. P. Desplans, Application of high sampling rate downhole measurements for analysis and cure of stick-slip in drilling, *SPE Annual Technical Conference and Exhibition*, 1994. https://doi.org/10.2118/28324-MS
11. T. Richard, C. Germay, E. Detournay, Self-excited stick-slip oscillations of drill bits, *Comptes Rendus. Mécanique*, 2004, 619–626. https://doi.org/10.1016/j.crme.2004.01.016
12. D. Forrest, C. Tibrea, M. Wang, M. Almodaris, S. Buddhi-Baedya, E. A. Carrasco, et al., Frequency analysis of surface and downhole dynamics demonstrates effectiveness of impedance matching torsional damping system across multiple drillstring harmonics, *SPE Annual Technical Conference and Exhibition*, 2025. https://doi.org/10.2118/227939-MS
13. M. Z. Doghmane, Influences of the stiffness and damping parameters on the torsional vibrations' severity in petroleum drilling systems, *Energies*, **18** (2025), 3701. https://doi.org/10.3390/en18143701
14. Y. A. Khulief, F. A. Al-Sulaiman, S. Bashmal, Vibration analysis of drillstrings with self-excited stick–slip oscillations, *J. Sound Vib.*, **299** (2007), 540–558. https://doi.org/10.1016/j.jsv.2006.06.065
15. N. Mihajlović, A. A. van Veggel, N. van de Wouw, H. Nijmeijer, Friction-induced torsional vibrations in an experimental drill-string system, *Proceedings of the 23rd IASTED International Conference on Modelling, Identification, and Control*, 2004.
16. T. Richard, C. Germay, E. Detournay, A simplified model to explore the root cause of stick-slip vibrations in drilling systems with drag bits, *J. Sound Vib.*, **305** (2007), 432–456. https://doi.org/10.1016/j.jsv.2007.04.015
17. X. Zheng, V. Agarwal, B. Balachandran, State-dependent delay effect in drilling, *Proceedings of the Fourth International Colloquium on Nonlinear Dynamics and Control of Deep Drilling Systems*, 2018.

18. F. F. Real, A. Batou, T. G. Ritto, C. Desceliers, R. R. Aguiar, Hysteretic bit/rock interaction model to analyze the torsional dynamics of a drill string, *Mech. Syst. Signal Process.*, **111** (2018), 222–233. https://doi.org/10.1016/j.ymssp.2018.04.014
19. J. Cao, D. Zou, Q. Xue, J. Wang, L. Huang, F. Guo, Analysis on the dynamics of flexible drillstring under different drilling parameters, *Front. Earth Sci.*, **12** (2024), 1396784. https://doi.org/10.3389/feart.2024.1396784
20. R. J. Shor, U. J. F. Aarsnes, F. di Meglio, Effects of latency, motor inertia and filtering on stick–slip mitigation control, *Nonlinear Dyn. Control Deep Drill. Syst.*, **133** (2018), 11–20.
21. L. C. de Barros, M. M. Lopes, F. S. Pedro, E. Esmi, J. P. C. Santos, D. E. Sánchez, The memory effect on fractional calculus: an application in the spread of COVID-19, *Comput. Appl. Math.*, **40** (2021), 72. https://doi.org/10.1007/s40314-021-01456-z
22. G. K. Hailu, S. W. Teklu, Improving passengers' attitudes toward safety and unreliable train operations: analysis of a mathematical model of fractional order, *Front. Appl. Math. Stat.*, **10** (2024), 1290494. https://doi.org/10.3389/fams.2024.1290494
23. V. E. Tarasov, General fractional economic dynamics with memory, *Mathematics*, **12** (2024), 2411. https://doi.org/10.3390/math12152411
24. J. A. Cunha, C. Soize, R. Sampaio, Computational modeling of the nonlinear stochastic dynamics of horizontal drillstrings, *Comput. Mech.*, **56** (2015), 849–878. https://doi.org/10.1007/s00466-015-1206-6
25. V. E. Tarasov, *Fractional dynamics: applications of fractional calculus to dynamics of particles, fields and media*, Springer, 2010. https://doi.org/10.1007/978-3-642-14003-7
26. S. Boulaaras, R. Jan, V. T. Pham, Recent advancement of fractional calculus and its applications in physical systems, *Eur. Phys. J. Special Top.*, **232** (2023), 2347–2350. https://doi.org/10.1140/epjs/s11734-023-01002-4
27. M. Caputo, M. Fabrizio, A new definition of fractional derivative without singular kernel, *Progress Fractional Differ. Appl.*, **1** (2015), 73–85. https://doi.org/10.12785/pfda/010201
28. A. Alkan, H. Anaç, A new study on the Newell-Whitehead-Segel equation with Caputo–Fabrizio fractional derivative, *AIMS Math.*, **9** (2024), 27979–27997. https://doi.org/10.3934/math.20241358
29. A. E. Abouelregal, A. H. Sofiyev, H. M. Sedighi, M. A. Fahmy, Generalized heat equation with the Caputo–Fabrizio fractional derivative for a nonsimple thermoelastic cylinder with temperature-dependent properties, *Phys. Mesomech.*, **26** (2023), 224–240. https://doi.org/10.1134/S1029959923020108
30. A. Alkan, H. Bulut, The numerical analysis of Caputo–Fabrizio fractional mathematical model of cancer chemotherapy, *Comput. Biol. Chem.*, **120** (2025) 108720. https://doi.org/10.1016/j.compbiolchem.2025.108720
31. Y. Sahin, M. Merdan, P. Açıkgöz, Development of a hybrid technique for solving the Newell–Whitehead–Segel equation using the Caputo–Fabrizio derivative, *Eng. Comput.*, 2025. https://doi.org/10.1108/EC-04-2025-0369
32. D. Baleanu, B. Shiri, Numerical solution for fractional Neumann series equations, *Ain Shams Eng. J.*, **17** (2026), 103915.
33. T. M. Atanacković, S. Pilipović, D. Zorica, Properties of the Caputo–Fabrizio fractional derivative and its distributional settings, *Fractional Calculus Appl. Anal.*, **21** (2018), 29–44. https://doi.org/10.1515/fca-2018-0003

34. A. Alshabanat, M. Jleli, S. Kumar, B. Samet, Generalization of Caputo–Fabrizio fractional derivative and applications to electrical circuits, *Front. Phys.*, **8** (2020), 64. https://doi.org/10.3389/fphy.2020.00064
35. J. Hristov, Transient heat diffusion with a non-singular fading memory: from the Cattaneo constitutive equation with Jeffrey's kernel to the Caputo–Fabrizio time-fractional derivative, *Therm. Sci.*, **20** (2016), 757–762. https://doi.org/10.2298/TSCI160112019H
36. X. Guo, S. Xiao, X. Qiu, X. Li, N. Hu, L. Dai, Experimental investigation on axial–torsional coupling nonlinear vibration characteristics of multi-body drill string system in oil and gas wells, *Nonlinear Dyn*., **113** (2025), 19401–19434. https://doi.org/10.1007/s11071-025-11159-3
37. G. Zheng, N. Zhang, S. Lv, The application of fractional derivative viscoelastic models in the finite element method: taking several common models as examples, *Fractal Fract.*, **8** (2024), 103. https://doi.org/10.3390/fractalfract8020103
38. F. Mainardi, *Fractional calculus and waves in linear viscoelasticity: an introduction to mathematical models*, Imperial College Press, 2010.
39. M. Wiercigroch, K. Nandakumar, L. Pei, M. Kapitaniak, V. Vaziri, *State dependent delayed drill-string vibration: theory, experiments and new model*, Procedia IUTAM, 2017, 39–50. https://doi.org/10.1016/j.piutam.2017.08.007
40. C. Germay, V. Denoël, E. Detournay, Multiple mode analysis of the self-excited vibrations of rotary drilling systems, *J. Sound Vib.*, **325** (2009), 362–381. https://doi.org/10.1016/j.jsv.2009.03.017
41. K. A. Abro, S. Qureshi, A. Atangana, Mathematical and numerical optimality of non-singular fractional approaches on free and forced linear oscillator, *Nonlinear Eng.*, **9** (2020), 449–456. https://doi.org/10.1515/nleng-2020-0028
42. A. Atangana, D. Baleanu, New fractional derivatives with nonlocal and nonsingular kernel: Theory and application to heat transfer model, *Thermal Sci.*, **20** (2016), 763–769. https://doi.org/10.2298/TSCI160111018A
43. S. Ghaderi, A. Heydari, S. Effati, Solving the fractional optimal control of a spring-mass-viscodamper system with Caputo–Fabrizio fractional operator, *Iran. J. Sci. Technol. Trans. Sci.*, **45** (2021), 247–257. https://doi.org/10.1007/s40995-020-01045-5
44. A. Alkan, Analysis of fractional advection equation with improved homotopy analysis method, *Osmaniye Korkut Ata Üniv. Fen Bilimleri Enstitüsü Derg.*, **7** (2024), 1215–1229. https://doi.org/10.47495/okufbed.1387630
45. M. S. Rawashdeh, The fractional natural decomposition method: theories and applications, *Math. Methods Appl. Sci.*, **40** (2017), 2362–2376. https://doi.org/10.1002/mma.4144
46. T. M. Elzaki, The new integral transform Elzaki transform, *Global J. Pure Appl. Math.*, **7** (2011), 57–64.
47. J. Singh, D. Kumar, R. Swroop, Numerical solution of time-and space-fractional coupled Burgers' equations via homotopy algorithm, *Alex. Eng. J.*, **55** (2016), 1753–1763. https://doi.org/10.1016/j.aej.2016.03.028
48. P. Veeresha, D. G. Prakasha, Solution for fractional Zakharov–Kuznetsov equations by using two techniques, *Chin. J. Phys.*, **60** (2019), 313–330. https://doi.org/10.1016/j.cjph.2019.05.009
49. K. A. Abro, A. Atangana, Numerical and mathematical analysis of induction motor by means of AB–fractal–fractional differentiation actuated by drilling system, *Numer. Methods Partial Differ. Equations*, **38** (2022), 293–307. https://doi.org/10.1002/num.22618
50. S. Zheng, Y. Lou, S. Shen, J. Lu, Numerical investigation of fractal oscillator for a pendulum with a rolling wheel, *Fractals*, **33** (2025), 1–11. https://doi.org/10.1142/S0218348X2550077X

51. L. Jin, S. Shen, J. Lu, L. Chen, S. Li, Numerical analysis of a fractional rotating pendulum oscillator, *Fractals*, **34** (2026), 2650064. https://doi.org/10.1142/S0218348X26500647
52. Y. Lou, J. Lu, M. Chen, L. Ma, H. Wang, Analytical approaches to fractal oscillator for a pendulum with a rolling wheel, *J. Low Freq. Noise Vib. Act. Control*, **45** (2025), 642–653. https://doi.org/10.1177/14613484251413080
53. S. Zheng, L. Chen, J. Lu, Numerical analysis of a fractional micro/nanobeam-based micro-electromechanical system, *Fractals*, **33** (2025), 1–10. https://doi.org/10.1142/S0218348X25500288
54. N. Almutairi, S. Saber, On chaos control of nonlinear fractional Newton–Leipnik system via fractional Caputo–Fabrizio derivatives, *Sci. Rep.*, **13** (2023), 22726. https://doi.org/10.1038/s41598-023-49541-z
55. M. Alhazmi, F. M. Dawalbait, A. Aljohani, K. O. Taha, H. D. Adam, S. Saber, Numerical approximation method and chaos for a chaotic system in sense of Caputo–Fabrizio operator, *Therm. Sci.*, **28** (2024), 5161–5168. https://doi.org/10.2298/TSCI2406161A
56. S. Saber, A. Alahmari, Existence, stability, and control of glucose-insulin dynamics via Caputo–Fabrizio fractal-fractional operators, *MethodsX*, **16** (2025), 103757. https://doi.org/10.1016/j.mex.2025.103757
57. H. D. Adam, M. Althubyani, S. M. Mirgani, S. Saber, An application of Newton's interpolation polynomials to the zoonotic disease transmission between humans and baboons system based on a time-fractal fractional derivative with a power-law kernel, *AIP Adv.*, **15** (2025), 045217. https://doi.org/10.1063/5.0253869

AIMS Press